



Preliminary Work for Preparation and Characterization of Anode Supported SOFC Based on NiO-YSZ Material Using Pore-Former

Muhammad Faesal Febriandyono¹, Sulistyto Sulistyto^{1*}, Ajie Muhamad Hertriyanto¹, Mohammad David Setyawan¹, Reza Abdu Rahman^{1,2}

¹ Department of Mechanical Engineering, Diponegoro University, Semarang 50275, Indonesia

² Department of Mechanical Engineering, Faculty of Engineering, Universitas Pancasila, Jagakarsa 12640, Indonesia

Corresponding Author Email: sulistyo@lecturer.undip.ac.id

Copyright: ©2024 The authors. This article is published by IIETA and is licensed under the CC BY 4.0 license (<http://creativecommons.org/licenses/by/4.0/>).

<https://doi.org/10.18280/rcma.340402>

ABSTRACT

Received: 18 May 2024
Revised: 10 July 2024
Accepted: 20 July 2024
Available online: 27 August 2024

Keywords:

nickel oxide, anode manufacturing, fuel cell, permeability, porosity

The present work assesses the manufacturing method for producing ceramic-based solid oxide fuel cells (SOFC) using compaction and sintering methods, which are combined by adding pore former to improve the porosity of the produced anode. The ratio of pore former varies between 5%, 10% and 15%. The base cermet material in this work is NiO-YSZ (Nickel Oxide/Yttria Stabilized Zirconia), which is suitable for high-temperature SOFC. The base material is mixed with pore former at the given ratio, followed by ultrasonic cleaning. This work uses polyethylene glycol (PEG, 10%) as binder material. The produced slurry is then dried in electric oven, continued with the compaction process at a pressure of 135MPa and sintered for 4 hours at 1200°C. The addition of pore former leads to significant improvement in the porosity level, with the highest value of 16.67%. It contributes to the excellent performance of the produced anode, particularly for the permeability value. The NiO-YSZ with 15% pore former has the highest permeability value with average of 0.37 m². Moreover, the detailed permeability profile shows the baseline ratio for adding pore former is between 5% and 10%, which experiences significant variation in the porosity level and permeability value.

1. INTRODUCTION

The high production and consumption of conventional energy sources severely impact the environment due to carbon emissions from the combustion process of fossil fuel. The development of renewable energy systems for grid energy production and utilization of alternative fuel has escalated significantly to solve the problem related to conventional energy sources [1-3]. The produced energy is used for power production, including the possibility of producing hydrogen. It makes a new path for processing hydrogen from green energy. The hydrogen itself is already taken as the main idea for building a hydrogen-based society. It can be applied for mobile and stationary applications to produce electricity using fuel cell technology [4]. The produced hydrogen can be stored, offering alternative storage systems besides electricity, mechanical and thermal [5]. Thus, fuel cell technology is highly applicable to the modern energy system.

Among various models of fuel cells, solid oxide fuel cell (SOFC) has many technical advantages [6], particularly for the working temperature, which reaches 1000°C. It improves the operational aspect since the system can operate effectively without additional effort to maintain the liquid concentration as commonly found for the liquid-based fuel cell [7]. The high operation temperature of the SOFC is achieved by using ceramic-based material, which prevents steam condensation

during the operation [8]. The ceramic-based SOFC requires suitable porosity between 20-40% to maintain the gas distribution between the anode and cathode [9]. The system operates continuously, involving heat, mass transfer, and electron transfer to the load in the form of electricity [10]. Therefore, the output of the system depends on the conversion rate of the hydrogen and oxygen, which is highly affected by the performance of the SOFC.

The development of SOFC is generally taken between the anode, cathode and electrolyte types, where each part offers various considerations [11]. For example, the anode-supported SOFC improves electrical conductivity but is considerably expensive, making it economically unfeasible [12]. Alternatively, the supported anode commonly uses a ceramic-metal (cermet) composite [13]. The cermet anode is an excellent combination to provide suitable conductivity and oxygen vacancies to initiate the reaction [14]. Choolaei et al. [15] employed Ceria-based SOFC, where the modification was made using nano-crystalline to adjust the temperature operation at the desired level. The high flexibility of cermet-based anode leads to a substantial achievement in using different materials such as NiO/YSZ (Nickel Oxide/Yttria Stabilized Zirconia) that is suitable for high-temperature operation at about 1000°C [16].

The production of anode-supported NiO-YSZ requires specific technology to ensure suitable porosity. Rednyk et al.

[17] employed liquid plasma technique for NiO-YSZ to fabricate SOFC. The work used water and ethanol-based feedstock and revealed some variation in the porosity and density level of the synthesized NiO-YSZ. Another work reported here [18] proposed a new approach using 3D printing, indicating that the produced YSZ has a high density of more than 95%. Different work focused on the production of ultra-thin YSZ for SOFC. The study here [18] used the phase inversion method to produce ultra-thin YSZ, resulting in a high conversion of methane gas (around 55%).

Different manufacturing concepts are proposed to improve the applicability of the produced NiO-YSZ. Soydan et al. [19] proposed a thermo-extrusion and dip-coating approach for producing micro-tubular SOFC, highlighting the power density affected by the processing method, which can be reduced up to 24.3%. Timurkutluk [20] reported the novel manufacturing method using tape casting and isostatic pressing, showing that the produced SOFC has an optimum porosity of around 26% with a maximum output of 645mW/cm². Zhou et al. [21] processed the porous zirconia SOFC as an integrated system through an advanced inert process, where the produced SOFC indicated an excellent output of 683mW/cm². Each reported literature shows various SOFC production approaches, indicating that the method is still developing.

The simplification of the producing method is critical to ensure the optimum process for developing SOFC. It can be taken by considering different material modifications [22-24]. A study conducted by Han et al. addressed the compatibility aspect of producing NiO-YSZ for SOFC, indicating that the performance of the produced SOFC depended on the temperature and surface decoration [25]. Chi et al. [26] discussed in detail from the molecular dynamic perspective on the effect of porosity for sintered NiO-YSZ, demonstrating the possibility for the simplification of the producing method through sintering and compaction. Therefore, alternative producing methods can be explored more in detail to obtain a convenient approach for developing NiO-YSZ for SOFC.

The sintering process is considered the simplest method for producing NiO-YSZ for SOFC. The process is combined with compaction, forming laminated SOFC at the desired thickness [27]. However, the process has one critical disadvantage due to high-pressure compaction that hinders the formation of a porous profile of the produced anode. Surface decoration is applied to address the issue. For example, Kuterbekov et al. [28] explored in detail the effect of surface decoration and granulometric of the produced anode, showing that the addition of pore former contributes positively to the formation of porosity within the anode.

The sintering and compaction process, including the type of pore former, potentially affects the quality of the produced SOFC [29]. However, the detailed analysis and the relation of the producing method for NiO-YSZ for SOFC are rarely discussed in one combined aspect. The present work is intended to explore the effect of pore former on the performance of the NiO-YSZ anode-supported SOFC. The anode is produced through compaction, considering its high potential for large-scale processing. This work uses commercial flour as a pore former, considering its sustainability for producing anode-supported SOFC. As a preliminary work, the ratio of the flour is set at 5%, 10% and 15%. The reported findings from this work are expected to provide a fundamental aspect for further developing a low-cost approach for synthesizing NiO-YSZ anode-supported SOFC.

2. MATERIALS AND METHOD

Figure 1 displays the schematic process for producing NiO-YSZ anode-supported SOFC in this work. The process was started by mixing NiO (12-22 μm), YSZ (3-5 μm), and pore former (fine powder, 62 μm) at the given ratio. In addition, ethanol was added to the mixture, which acts as a solvent.

The mixture was fed into the ultrasonic cleaner machine and stirred at 100rpm to ensure the homogeneity of the slurry. After that, the homogenous slurry was put in the oven at a temperature of 100°C to remove the ethanol. The dried mixture was then mixed with polyethylene glycol (PEG, Aldrich), which was designed as a binder for the compaction process [30].

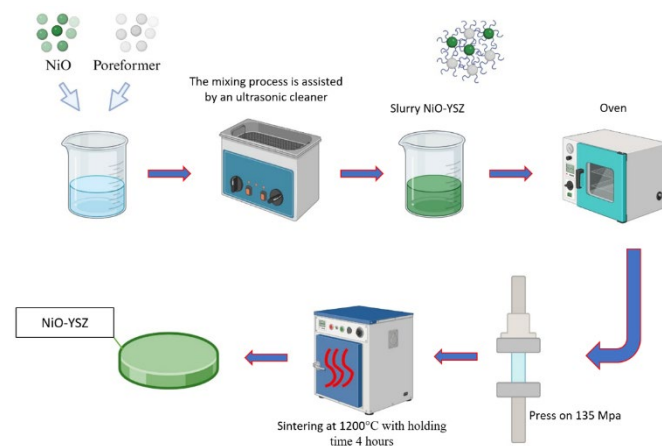


Figure 1. Schematic process for producing the NiO-YSZ anode-supported SOFC with pore former

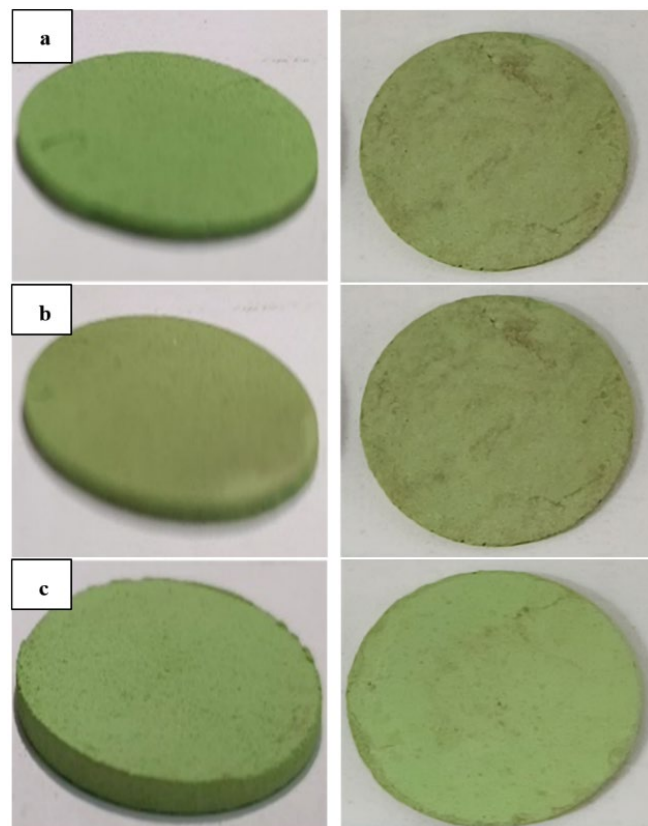


Figure 2. The produced sample from this work: (a) NiO-YSZ with 5% pore former; (b) NiO-YSZ with 10% pore former; (c) NiO-YSZ with 15% pore former

The mixture then processed into the compaction apparatus (hydraulic press) at a pressure of 130MPa. At the end of the compaction, the pellets were examined visually and checked for its dimension. If the pellet passed the initial quality check, it continued to the final step on the sintering furnace (Nabertherm) at a temperature of 1200°C with a holding time of 4 hours at a heating rate of 3°C/minutes [31]. The pellet was removed and checked for its quality and dimension before final characterization

Figure 2 shows the produced sample for NiO-YSZ with different pore-former ratios. The diameter of the produced NiO-YSZ is 25 mm, with thickness between 1-2 mm. The produced NiO-YSZ was in compact form, which is the main advantage for using SOFC. The produced NiO-YSZ then processed for further evaluation. The first evaluation was taken to measure the density level of the sample using density meter (Vibra). The key evaluation was performed using gas permeability tester for the produced sample. The value is plotted according to the average volumetric flowrate and pressure drop from the measurement. The measurement was repeated 11 times to ensure the quality of the evaluation.

3. RESULTS AND DISCUSSION

Figure 3 shows the density percentage of the produced sample. First, adding pore former clearly affects the decrement of density level for the produced anode. However, it shows a non-linear correlation since adding 5wt.% and 10wt.% causes a significant deviation in the density percentage of the sample. The density of NiO-10wt.% falls by about 8.13% compared to NiO-5wt.%, while the variation at higher concentrations (NiO-15wt.%) only reduces by 3.27% compared to NiO-10wt.%. The pore former produces more space at a higher ratio, leading to a notable decrease in density. According to the result, determining a suitable ratio of pore former must be addressed carefully, including factors that interfere during production, particularly for the compaction and sintering process.

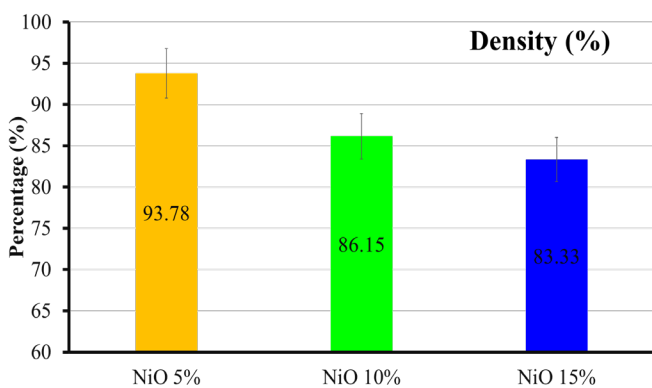


Figure 3. Density percentage of the produced NiO-YSZ sample

The formation of porosity percentage on the produced sample shows a great value according to the ratio of pore former. As plotted in Figure 4, the influence on the pore former ratio significantly improves the porosity percentage. The highest improvement is observed between 5wt.% and 10wt.%. It confirms that the formation of pore structure for the produced SOFC is controlled effectively by using pore former, in which a higher ratio of pore former leads to a considerable increment in the porosity level of the structure [32]. It is related

to the structural decoration of the anode, as adding a pore former creates an additional pathway for the gas to diffuse through the structure. Moreover, it proves that the produced anode with pore former through the compaction process is feasible to provide additional decoration within the laminated surface of the SOFC.

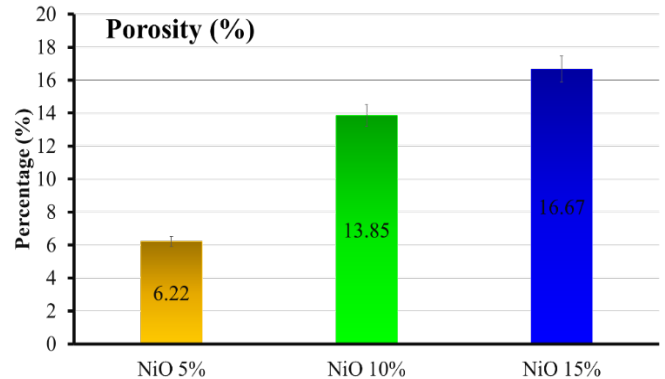


Figure 4. Density percentage of the produced NiO-YSZ sample

Figure 5 shows the data from the permeability measurement with a trendline $\pm 25\%$ according to ASTM D6539-13. Two outlier data were obtained from the measurement of permeability for NiO-YSZ 5%. It is affected by the airflow from the sample, which has non-laminar conditions [33]. It also reflects the pore characteristics of the produced anode, which directly relates to the pore structure and permeability value.

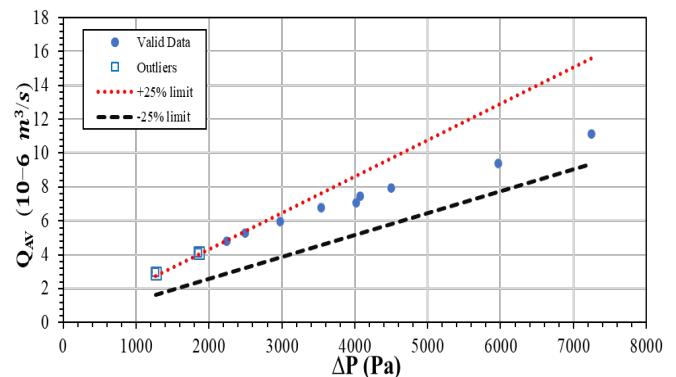


Figure 5. Anode gas permeability testing for NiO-YSZ 5%

Figure 6 shows the detailed permeability value for NiO-YSZ 5%. The profile indicates the permeability value decreases, which is proportional to the increment of the differential pressure. The initial profile shows the permeability can be maintained steadily up to 0.088 m² with a maximum differential pressure of 2310Pa (yellow box in Figure 6). However, it falls drastically until the pressure reaches 4740 Pa with a maximum permeability of 0.073 m². Interestingly, the value can be maintained (green box) before it drops to the lowest value (0.063 m²). The fluctuating profile is highly affected by the pore structure of the produced sample, which corresponds to the average porosity value (Figure 4). The lower permeability demonstrates that the diffusion path for the gas is undesirable, which may cause technical problems regarding the flux densities of the SOFC [34]. Moreover, the average permeability is considerably low at 0.076 m² with an average differential pressure of 4413.3Pa.

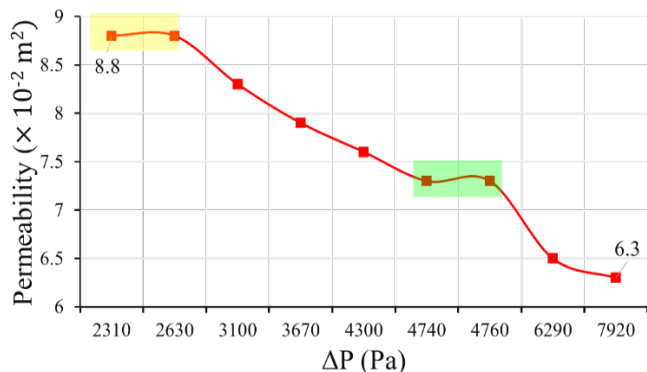


Figure 6. Detailed profile of permeability test for NiO-YSZ 5%

The effect of porosity level causes different results on the permeability profile value. As seen in Figure 7, the obtained data from NiO-YSZ 10% fits with the standard limitation. The measurement indicates the outlier data is only one, making the profile measurement for the NiO-YSZ 10% favorable. It is highly related to the porosity percentage of the sample (Figure 4) and confirms that the pore structure is obtained sufficiently.

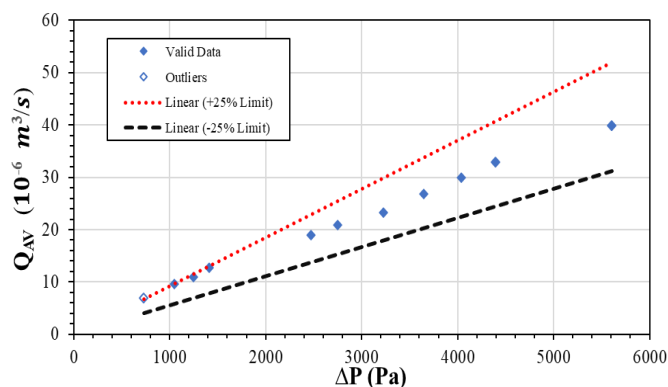


Figure 7. Anode gas permeability testing for NiO-YSZ 10%

The permeability profile for NiO-YSZ 10% differs notably from the previous profile of NiO-YSZ 5%. As plotted in Figure 8, the initial value of the permeability shows a fluctuation (red box) with an average permeability of 0.341 m^2 .

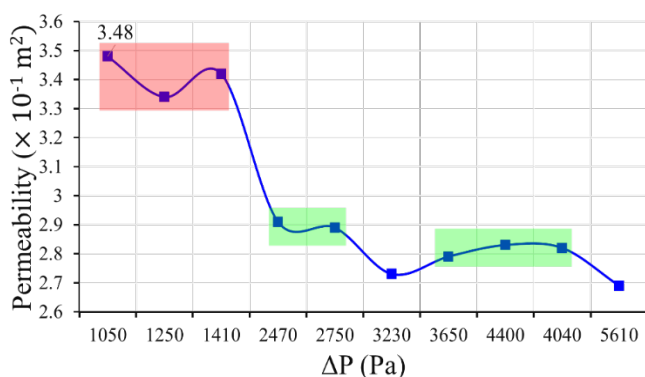


Figure 8. Anode gas permeability testing for NiO-YSZ 10%

As the process continues, the permeability decreases, showing a dual steady value (green box) at the given pressure range. According to the profile, the pore structure of the NiO-

YSZ 10% is achieved with suitable performance, confirming the high differences in density percentage compared to NiO-YSZ 5%. It indicates the addition of 10wt.% pore former shows a notable improvement in the performance of the SOFC, which also can be observed according to the higher permeability value for NiO-YSZ 10% (0.299 m^2). Despite the fluctuation, the differential pressure at the given region varies slightly, with a maximum deviation of 360 Pa. This indicates that the produced anode (NiO-YSZ 10%) is able to handle gas diffusion effectively without causing significant pressure differences. It is favorable for the SOFC system since the reaction path can be maintained effectively without causing significant pressure drop and potentially maintain the effective reaction process [35].

The permeability test for NiO-YSZ 15% shows a good value where the all-measured data is obtained at the acceptance range. The detailed permeability profile is plotted in Figure 9. It is the only sample that experiences a peak-valley profile, commonly found in a high diffusion gas ratio of the SOFC [36]. It highlights the excellent pore structure of the NiO-YSZ 15%, which potentially improves the performance of the SOFC. The initial permeability value is maintained steadily, similar to NiO-YSZ 5%. However, the NiO-YSZ 15% indicates a steady profile at the end of the measurement (blue box), in which the value varies slightly (around 0.2 m^2) compared to the initial value. Thus, it makes the produced sample highly suitable for the operation of SOFC, considering its excellent diffusion path with the lowest differential pressure (2638.2 Pa) compared to the other NiO-YSZ at different pore former ratios.

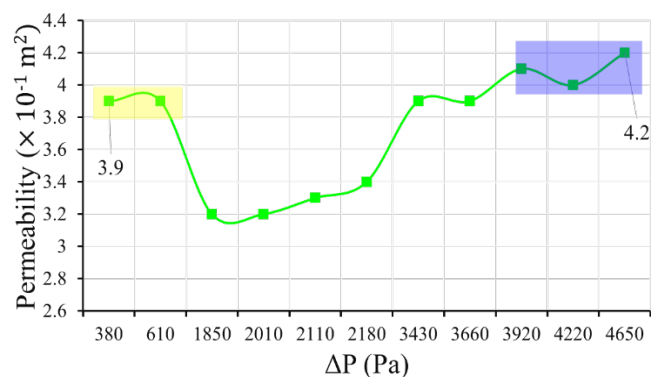


Figure 9. Detailed profile of permeability test for NiO-YSZ 15%

The higher pore former ratio causes a larger pore diameter for the NiO-YSZ. As observed in Figure 10(b), the NiO-YSZ 10% has a substantial pore diameter of around $472.58 \mu\text{m}^2$. This confirms the higher permeability value of NiO-YSZ 10% compared to NiO-YSZ 5% as shown in Figure 10(a). The observed pore diameter for NiO-YSZ 15% indicates the largest pore size Figure 10(c), confirming the highest permeability value for this sample. However, the morphology demonstrates the uneven distribution of pore-former, which should be addressed carefully during the production process. Despite the uneven distribution, the minimum ratio of 10 wt.% pore former can be set as the minimum level to ensure suitable permeability of the NiO-YSZ for SOFC.

The surface observation directly impacts the pore distribution, highlighting its impact on the permeability value of the produced anode. The porosity distribution within the anode provides multiple pathways for gas diffusion [37]. It is the main feature for using a higher pore former ratio, proving

that the compaction method is feasible to produce anode-supported SOFC. Thus, a simple manufacturing method combined with the addition of suitable pore former is applicable as a feasible option for producing anode SOFC. However, the study is limited to using one specific densification force and pore former, which requires further observation to assess the impact of different densification rates using various pore former.

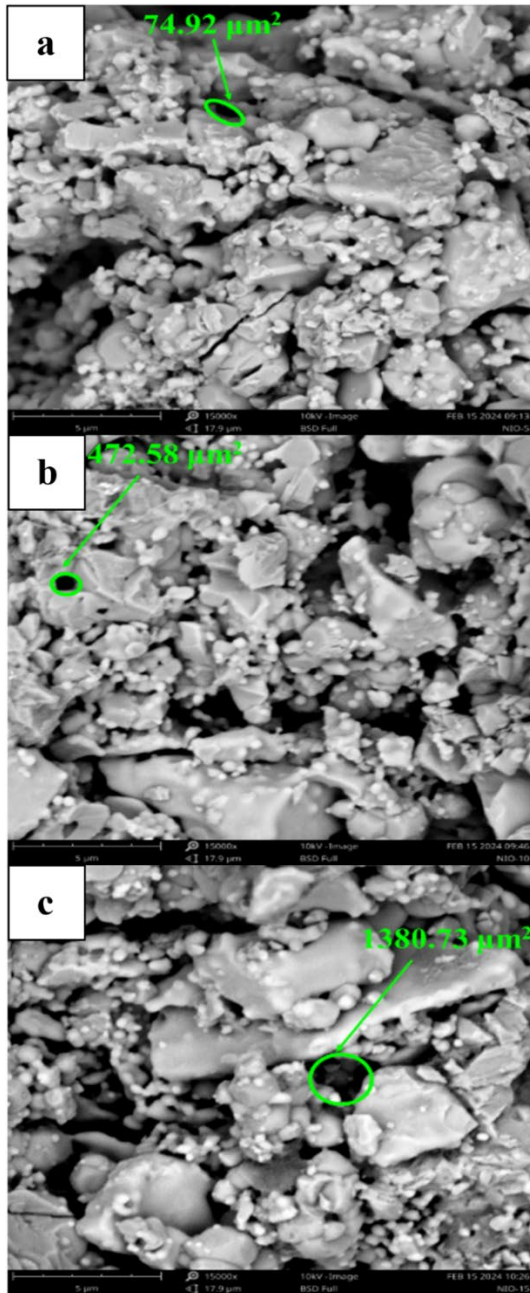


Figure 10. SEM profile for the evaluated NiO-YSZ with different pore former ratio: (a) NiO-YSZ with 5% pore former; (b) NiO-YSZ with 10% pore former; (c) NiO-YSZ with 15% pore former

4. CONCLUSION

The present work indicates a suitable method for producing NiO-YSZ anode-supported SOFC through compaction. Adding a pore former can minimize the technical barrier regarding the pore structure of the compacted anode. The

suitable ratio is obtained between 10wt.% and 15wt.% by considering the highest permeability value between 0.299 m²-0.373 m². The differential pressure for the given ratio is considerably low, with the lowest value of 2638.2Pa, making the applicability of the produced anode advisable for the high-temperature fuel cell. The surface observation implies that pore structure can be achieved through compaction, making it suitable for large-scale processing of anode SOFC.

One critical aspect is the high variation between pore former 5% and 10%, showing that the value is a non-linear profile. It makes further observations can be performed using the given ratio as the baseline, including the modification of the densification force for producing the anode. Moreover, the actual test can be taken using a fuel cell compartment to observe the power density of the produced anode. Despite that, a simple manufacturing method is feasible to be further explored and studied to ensure the applicability and usability of anode SOFC. Eventually, it will lead to sustainable technology for improving fuel cell operation as modern green technology equipment.

REFERENCES

- [1] Mehrjardi, S.A.A., Khademi, A., Fazli, M. (2024). Optimization of a thermal energy storage system enhanced with fins using generative adversarial networks method. *Thermal Science and Engineering Progress*, 49: 102471. <https://doi.org/10.1016/j.tsep.2024.102471>
- [2] Suyitno, B.M., Rahman, R.A., Sukma, H., Rahmalina, D. (2022). The assessment of reflector material durability for concentrated solar power based on environment exposure and accelerated aging test. *Eastern-European Journal of Enterprise Technologies*, 6(12): 120. <https://doi.org/10.15587/1729-4061.2022.265678>
- [3] Adji, R.B., Rahman, R.A. (2023). Increasing the feasibility and storage property of cellulose-based biomass by forming shape-stabilized briquette with hydrophobic compound. *Case Studies in Chemical and Environmental Engineering*, 8: 100443. <https://doi.org/10.1016/j.cscee.2023.100443>
- [4] Halder, P., Babaie, M., Salek, F., Shah, K., Stevanovic, S., Bodisco, T.A., Zare, A. (2024). Performance, emissions and economic analyses of hydrogen fuel cell vehicles. *Renewable and Sustainable Energy Reviews*, 199: 114543. <https://doi.org/10.1016/j.rser.2024.114543>
- [5] Rahmalina, D., Rahman, R.A. (2023). Hybrid energy-temperature method (HETM): A low-cost apparatus and reliable method for estimating the thermal capacity of solid-liquid phase change material for heat storage system. *HardwareX*, 16: e00496. <https://doi.org/10.1016/j.ohx.2023.e00496>
- [6] Adam, A., Fraga, E.S., Brett, D.J. (2018). A modelling study for the integration of a PEMFC micro-CHP in domestic building services design. *Applied Energy*, 225: 85-97. <https://doi.org/10.1016/j.apenergy.2018.03.066>
- [7] Timurkutluk, C., Bilgil, K., Celen, A., Onbilgin, S., Altan, T., Aydin, U. (2022). Experimental investigation on the effect of anode functional layer on the performance of anode supported micro-tubular SOFCs. *International Journal of Hydrogen Energy*, 47(45): 19741-19751. <https://doi.org/10.1016/j.ijhydene.2021.09.260>
- [8] Murutoglu, M., Ucu, T., Ulasan, O., Buyukaksoy, A., Tur, Y.K., Yilmaz, H. (2022). Cold sintering-assisted

- densification of GDC electrolytes for SOFC applications. *International Journal of Hydrogen Energy*, 47(45): 19772-19779.
<https://doi.org/10.1016/j.ijhydene.2022.01.043>
- [9] Wincewicz, K.C., Cooper, J.S. (2005). Taxonomies of SOFC material and manufacturing alternatives. *Journal of Power Sources*, 140(2): 280-296.
<https://doi.org/10.1016/j.jpowsour.2004.08.032>
- [10] Rath, M.K., Jung, Y.M., Park, J.H., Joh, D.W., Lee, K.T. (2017). Heterogeneous nanograin structured NiO-YSZ anodes via a water-in-oil microemulsion route for solid oxide fuel cells. *Journal of Alloys and Compounds*, 723: 681-688. <https://doi.org/10.1016/j.jallcom.2017.06.294>
- [11] Yang, H., Hanif, M.B., Zhang, S.L., Li, C.J., Li, C.X. (2021). Sintering behavior and electrochemical performance of A-site deficient $Sr_xTi_{1.3}Fe_{0.7}O_{3-\delta}$ oxygen electrodes for solid oxide electrochemical cells. *Ceramics International*, 47(17): 25051-25058.
<https://doi.org/10.1016/j.ceramint.2021.05.235>
- [12] Naeemakhtar, M., Manjanna, J. (2021). Ionic conductivity of $Ce_{0.91}Ca_{0.09}O_{2-\delta}$ as an electrolyte for intermediate temperature solid oxide fuel cells. *Research Journal of Chemistry and Environment*, 25(12): 1-9.
<https://doi.org/10.25303/2512rjce001009>
- [13] Sulistyono, S. (2015). Pengontrolan kualitas anode solid oxide fuel cell (sofc) melalui pengontrolan porositas. *Seminar Nasional Tahunan Teknik Mesin Indonesia XIV*. (2015): 7-8.
- [14] Shabri, H.A., Othman, M.H.D., Mohamed, M.A., Kurniawan, T.A., Jamil, S.M. (2021). Recent progress in metal-ceramic anode of solid oxide fuel cell for direct hydrocarbon fuel utilization: A review. *Fuel Processing Technology*, 212: 106626.
<https://doi.org/10.1016/j.fuproc.2020.106626>
- [15] Choolaei, M., Jakubczyk, E., Horri, B.A. (2023). Synthesis and characterisation of a ceria-based cobalt-zinc anode nanocomposite for low-temperature solid oxide fuel cells (LT-SOFCs). *Electrochimica Acta*, 445: 142057. <https://doi.org/10.1016/j.electacta.2023.142057>
- [16] Niazmand, M., Maghsoudipour, A., Alizadeh, M., Khakpour, Z., Kariminejad, A. (2022). Effect of dip coating parameters on microstructure and thickness of 8YSZ electrolyte coated on NiO-YSZ by sol-gel process for SOFCs applications. *Ceramics International*, 48(11): 16091-16098.
<https://doi.org/10.1016/j.ceramint.2022.02.155>
- [17] Rednyk, A., Musalek, R., Tesar, T., Medricky, J., Tsepeleva, A., Lukac, F., Ctibor, P., Sedlacek, J., Chraska, T. (2024). Liquid plasma spraying of NiO-YSZ anode layers applicable for SOFC. *Materials Today Communications*, 38: 107855.
<https://doi.org/10.1016/j.mtcomm.2023.107855>
- [18] Wang, T., Sun, N., Wang, R., Chen, D., Dong, D., Shen, X., Wei, T., Wang, Z. (2024). One-step preparation of large-size 1.5- μ m-thick robust YSZ electrolyte for high CH_4 conversion SOFCs at 600°C. *Separation and Purification Technology*, 349: 127825.
<https://doi.org/10.1016/j.seppur.2024.127825>
- [19] Soydan, A.M., Yıldız, Ö., Durğun, A., Akduman, O.Y., Ata, A. (2019). Production, performance and cost analysis of anode-supported NiO-YSZ micro-tubular SOFCs. *International Journal of Hydrogen Energy*, 44(57): 30339-30347.
<https://doi.org/10.1016/j.ijhydene.2019.09.156>
- [20] Timurkutluk, C. (2023). Development of functionally graded anode supports for microtubular solid oxide fuel cells by tape casting and isostatic pressing. *International Journal of Hydrogen Energy*, 48(46): 17641-17653.
<https://doi.org/10.1016/j.ijhydene.2023.01.249>
- [21] Zhou, X., Wang, J., Pang, X., Guo, X., Zhao, Z., Sunarso, J., Yu, F., Meng, X., Zhang, J., Yang, N. (2024). Integrated micro-tubular SOFC stack supported by a monolithic porous zirconia prepared using 3D printing technology. *Journal of the European Ceramic Society*, 44(13): 7837-7845.
<https://doi.org/10.1016/j.jeurceramsoc.2024.05.060>
- [22] Somacescu, S., Cioatera, N., Osiceanu, P., Calderon-Moreno, J.M., Ghica, C., Neațu, F., Florea, M. (2019). Bimodal mesoporous NiO/CeO₂- δ -YSZ with enhanced carbon tolerance in catalytic partial oxidation of methane-Potential IT-SOFCs anode. *Applied Catalysis B: Environmental*, 241: 393-406.
<https://doi.org/10.1016/j.apcatb.2018.09.065>
- [23] Suyitno, B.M., Anggrainy, R., Plamonia, N., Rahman, R.A. (2023). Preliminary characterization and thermal evaluation of a direct contact cascaded immiscible inorganic salt/high-density polyethylene as moderate temperature heat storage material. *Results in Materials*, 19: 100443.
<https://doi.org/10.1016/j.rinma.2023.100443>
- [24] Zhao, X., Xiao, L., Pan, B., Yuan, J. (2023). Modeling and prediction of structural/thermophysical properties of sintered NiO/YSZ anode for SOFC by molecular dynamics method. *Journal of Alloys and Compounds*, 958: 170502.
<https://doi.org/10.1016/j.jallcom.2023.170502>
- [25] Han, Z., Dong, H., Wang, H., Yang, Y., Yu, H., Yang, Z. (2023). Temperature-dependent chemical incompatibility between NiO-YSZ anode and alkaline earth metal oxides: Implications for surface decoration of SOFC anode. *Journal of Alloys and Compounds*, 968: 172150. <https://doi.org/10.1016/j.jallcom.2023.172150>
- [26] Chi, H., Xiao, L., Deng, T., Pan, B., Yuan, J. (2024). Modeling and characterization of sintered YSZ/NiO porous electrode structural properties using coarse-graining molecular dynamics method. *Ceramics International*, 50(14): 26205-26219.
<https://doi.org/10.1016/j.ceramint.2024.04.361>
- [27] Gao, B., Liu, Z., Ji, S., Ao, Q. (2022). Fabrication of a YSZ electrolyte layer via co-pressing/co-sintering for tubular NiO-YSZ anode-supported SOFCs. *Materials Letters*, 323: 132547.
<https://doi.org/10.1016/j.matlet.2022.132547>
- [28] Kuterbekov, K., Nikonov, A., Bekmyrza, K., Khrustov, V., Pavzderin, N., Kabyshev, A., Kubenova, M. (2024). Co-sintering of gradient anode-electrolyte structure for microtubular SOFC. *Ceramics International*, 50(10): 17242-17251.
<https://doi.org/10.1016/j.ceramint.2024.02.199>
- [29] Cigdem, T., Onbilgin, S., Timurkutluk, B., Pamuk, I. (2022). Effects of pore former type on mechanical and electrochemical performance of anode support microtubes in solid oxide fuel cells. *International Journal of Hydrogen Energy*, 47(22): 11633-11643.
<https://doi.org/10.1016/j.ijhydene.2022.01.178>
- [30] Talebi, T., Sarrafi, M.H., Haji, M., Raissi, B., Maghsoudipour, A. (2010). Investigation on microstructures of NiO-YSZ composite and Ni-YSZ

- cermet for SOFCs. *International Journal of Hydrogen Energy*, 35(17): 9440-9447. <https://doi.org/10.1016/j.ijhydene.2010.04.156>
- [31] Hong, J.E., Ida, S., Ishihara, T. (2014). Effects of transition metal addition on sintering and electrical conductivity of La-doped CeO₂ as buffer layer for doped LaGaO₃ electrolyte film. *Solid State Ionics*, 262: 374-377. <https://doi.org/10.1016/j.ssi.2013.11.049>
- [32] Han, Z., Dong, H., Yang, Y., Yu, H., Yang, Z. (2024). Novel BaO-decorated carbon-tolerant Ni-YSZ anode fabricated by an efficient phase inversion-impregnation approach. *Journal of Power Sources*, 591: 233869. <https://doi.org/10.1016/j.jpowsour.2023.233869>
- [33] Nickerson, S., Shu, Y., Zhong, D., Könke, C., Tandia, A. (2019). Permeability of porous ceramics by X-ray CT image analysis. *Acta Materialia*, 172: 121-130. <https://doi.org/10.1016/j.actamat.2019.04.053>
- [34] Naouar, A., Ferrero, D., Santarelli, M., Dhahri, H., Mhimid, A. (2024). Numerical study of electrode permeability influence on planar SOFC performance. *International Journal of Hydrogen Energy*, 78: 189-201. <https://doi.org/10.1016/j.ijhydene.2024.06.274>
- [35] Ung-arphorn, Y., Yeyongchaiwat, J., Chaianansutcharit, S. (2024). Oxygen permeability and electrochemical performance of Ca-doped NdBaCo₂O_{5+δ} in IT-SOFC. *Journal of Alloys and Compounds*, 991: 174468. <https://doi.org/10.1016/j.jallcom.2024.174468>
- [36] Shi, A., Kong, Y., Li, Z., Wang, Y., Fan, S., Jin, Z. (2023). Performance analysis of series connected cathode supported tubular SOFCs. *International Journal of Electrochemical Science*, 18(5): 100126. <https://doi.org/10.1016/j.ijoes.2023.100126>
- [37] Shirasangi, R., Dasari, H. P., & Saidutta, M. B. (2024). Current-Voltage (iV) characteristics of electrolyte-supported (NiO-YSZ/NiO-SDC/ScSZ/LSCF-GDC/LSCF) solid oxide electrolysis cell during CO₂/H₂O co-electrolysis. *Chemical Physics Impact*, 100670. <https://doi.org/10.1016/j.chphi.2024.100670>